

SECOND ORDER WAVE INTERACTION WITH A LARGE STRUCTURE

Bjarne Büchmann ¹, Jesper Skourup ² and David L. Kriebel ³

Abstract

Wave diffraction around a large vertical circular bottom mounted cylinder is considered. Results from a 3D second-order numerical time domain Boundary Element Model, a 3D second-order semi-analytical frequency domain model and experiments are compared and show good agreement over a wide range of wave frequencies and wave steepnesses. In general the agreement between the calculated and experimental results is satisfactory even in some cases where second-order Stokes' wave theory is not *a priori* expected to provide accurate results. The two numerical models have thus been validated against each other and validated against experiments. It is noted that the inclusion of second-order effects is important for the accurate estimation of run-up on a structure.

1 INTRODUCTION

Wave interaction with a large cylindrical structure is considered. The Keulegan-Carpenter number is small and thus inertial effects are dominant. Hence, potential theory can be applied. Conventional methods for estimating the influence on the wave field due to the presence of a large structure are often based on linear wave theory. However, second-order effects may be important and can lead to a significant increase of *e.g.* the run-up on a structure when compared to run-up calculated using linear theory. In the present paper a 3D time domain Boundary Element Model (BEM) correct to second order (see Büchmann *et al.*, 1998) is used for simulating the three dimensional interaction between waves and a structure. Comparisons are made with the run-up envelope results from the second-order semi-analytical frequency domain model by Kriebel (1990) as well as with experimental results by Kriebel (1992) for all the test cases considered by Kriebel (1992). Comparisons are also made to the well known first-order solution by MacCamy and Fuchs (1954) (see Skourup and Bingham, 1996, for further first order comparisons.)

¹Department of Hydrodynamics and Water Resources (ISVA), DTU, DK-2800 Lyngby, Denmark

²International Research Centre for Computational Hydrodynamics (ICCH), Danish Hydraulic Institute, Agern Allé 5, DK-2970 Hørsholm, Denmark

³NAOME Department, 590 Holloway Road, Annapolis, MD 21402, USA

2 NUMERICAL MODELS

The BEM is formulated and implemented up to second order with the wave steepness as perturbation parameter. The kinematic and dynamic free surface conditions are Taylor expanded about the mean free surface position and perturbation expansions are applied to the free surface elevation and to the velocity potential there. Hence, the boundary value problem is formulated at each order in a time-invariant geometry. The velocity potential and the free surface elevation are separated into incoming (known) and scattered components, and the boundary value problem at each order is then solved for the scattered parts alone. The scattered waves are all outgoing (of the domain) and the lateral boundary conditions can thus be formulated as radiation conditions. In the present work the lateral boundaries are modeled as active wave absorbers (as known from physical wave tank facilities). These may be used in combination with a sponge layer on the free surface in order to ensure an efficient absorption over a wide range of wave frequencies. Further details about the model can be found in Skourup (1996) and in Büchmann *et al.* (1998).

A closed-form frequency domain solution correct to second order for the diffraction of Stokes waves around a large vertical circular bottom mounted cylinder is given by Kriebel (1990). At first order the solution corresponds to the usual linear diffraction theory. At second order, however, the solution consists of a combination of forced waves due to the non-linear wave-wave interaction of the first order incident and scattered waves, and free waves due to the interactions of the forced waves with the cylinder. Further details about this semi-analytical frequency domain model can be found in Kriebel (1990, 1992).

3 STUDY PARAMETERS

Since both the numerical time domain model and the semi-analytical frequency domain model employ a Stokes' expansion method on the non-linear free surface conditions, it is expected that both models are limited to waves of small to medium wave steepness. Thus, it is appropriate to compare the wave steepness used in the experiments to the maximal wave steepness for the given frequency and water depth. Fenton (1990) gives a rational-function approximation for this maximum wave height by fitting to numerical results for progressive waves of maximum steepness.

$$\frac{H_{\max}}{h} = \frac{0.141063 \frac{L}{h} + 0.0095721 \left(\frac{L}{h}\right)^2 + 0.0077829 \left(\frac{L}{h}\right)^3}{1 + 0.0788340 \frac{L}{h} + 0.0317567 \left(\frac{L}{h}\right)^2 + 0.0093407 \left(\frac{L}{h}\right)^3} \quad (1)$$

Here H is the wave height, L is the wave length and h is the water depth. As a measure of the non-linearity of the wave the relative wave steepness, S , *i.e.* the wave steepness relative to the maximum steepness, can be introduced as

$$S(k, H) = \frac{kH}{(kH)_{\max}} = \frac{H}{H_{\max}} \quad (2)$$

where $k = 2\pi/L$ is the wave number.

It is well known that a secondary crest appears in the trough of the primary wave when Stokes' second-order theory is used for very steep waves. This is often used as an upper

limit to this theory by imposing a “no secondary crest” condition. For progressive waves of permanent form the condition can be written as

$$\left(\frac{H}{L}\right)_{\max} = \frac{1}{4f_{\eta}(kh)} \quad , \quad f_{\eta}(kh) = \frac{\pi}{4}(3 \coth^3 kh - \coth kh) \quad (3)$$

see *e.g.* Svendsen and Jonsson (1980) for details. Equivalently the ratio, a^{21} , between the second-order wave amplitude and the linear wave amplitude can be used to limit the theory. The “no secondary crest” condition then corresponds to $a^{21} < 0.25$. For progressive Stokes waves of permanent form a^{21} is

$$a^{21} = \frac{1}{8}kH(3 \coth^3 kh - \coth kh) \quad (4)$$

It should be noted that the second-order Stokes’ progressive wave theory may show considerable error when compared to *e.g.* the stream function wave theory even without violating the limit $a^{21} < 0.25$.

For a blunt body in waves a partially standing wave system is located in front of the structure. Thus it may be more appropriate to use the “no secondary crest” condition for Stokes’ second-order standing waves as an upper limit. The criterion for plane standing waves is somewhat more restrictive than for progressive waves, especially in deeper waters, and can be expressed as *e.g.*

$$\left(\frac{H^{(s)}}{L}\right)_{\max} = \frac{1}{4f_{\eta}^{(s)}(kh)} \quad , \quad f_{\eta}^{(s)}(kh) = \frac{\pi}{4}(3 \coth^3 kh - \coth kh + 2 \coth 2kh) \quad (5)$$

where $H^{(s)}$ is the height of the incident wave.

It is evident that numerical models based on Stokes’ theory should not be employed to model waves in the cnoidal wave regime. The Ursell parameter $U = HL^2/h^3$ can be used as an indication of the wave regime. Thus, for H/h larger than, say, 10% an Ursell parameter $U = 40$ can be used to divide the Stokes’ waves regime from the cnoidal waves regime.

The Keulegan-Carpenter number, KC , is an important parameter for indication of the relative importance of viscous effects. A value of KC less than about two to three indicates that viscous effects are not of importance for wave–structure interaction. Using linear Stokes theory at the mean water level to predict the maximum horizontal velocity, u_{\max} , KC can be written on the form

$$KC = \frac{u_{\max}T}{2a} = \frac{\pi}{2} \frac{kH}{ka \tanh kh} \quad (6)$$

where T is the wave period and a is the radius of the cylinder.

4 EXPERIMENTS

Kriebel (1992) conducted a series of experiments to find the run-up around the circumference of a vertical circular bottom mounted cylinder in various regular wave conditions. A

definition sketch showing the geometry and main variables is given in Figure 1. The test conditions ranged from fairly low wave steepness to very steep waves where wave breaking around the cylinder was observed. In some cases super-critical run-up occurred in the form of a vertical jet on the cylinder. Since the potential theory models considered in this work are limited to non-breaking waves, these test cases are not considered in detail here. Also in the cases where breaking was observed in the experiments the agreement between the two second-order numerical models is good, but the results deviate significantly from the results found in the experiments.

In Table 1 the parameters for the test cases considered are given. In addition to parameters mentioned previously, the ratio of the cylinder diameter, D , to the wave length is also given:

$$D/L = ka/\pi \tag{7}$$

It is noted from Table 1 that the Keulegan-Carpenter number KC is small in all the test cases considered. Thus, it is expected that inertial effects are predominant and potential theory can be applied.

To give an overview of the range of wave conditions used, a scatter diagram of the wave height relative to the water depth against the wave length relative to the water depth is

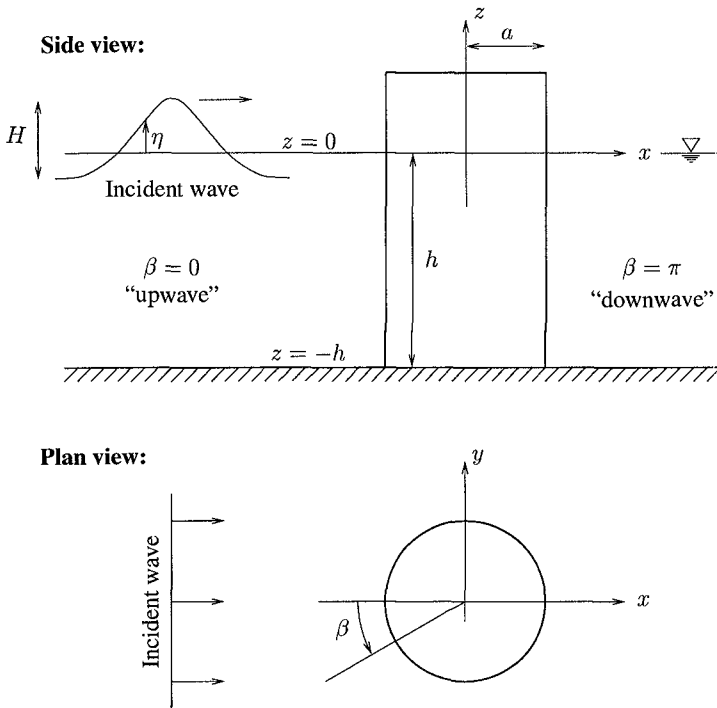


Figure 1: Definition sketch.

depicted in Figure 2. It is noted that the waves are very close to breaking in a few of the cases. In the cases used in this work (shown with squares) the relative wave steepness, S , varies from 15% to 72% (see also Table 1). It is noted that the "no secondary crest" condition for progressive second-order Stokes waves (3) is violated in three of the test cases used, while in many of the cases this limit is exceeded using the standing wave criterion (5). Thus it is clear that in many of the test cases it would be appropriate to use a model based on a Stokes theory of order larger than two, or even a model based on a fully non-linear wave theory. Therefore, the present study also gives indications of the validity range of the two numerical models.

5 RESULTS

Using the time domain BEM the influence on the wave field due to the presence of a fixed structure is computed as mean values over some wave periods. The parts of the time series where initial conditions or reflections from the lateral boundaries can be seen are not used. The run-up on a bottom mounted vertical circular cylinder is calculated in this paper, but this specific shape of the structure is not a restriction to the BEM. The wave run-up is

Figure	ka	kh	kH	S	KC	a^{21}	D/L
3a	0.271	0.750	0.132	0.257	1.20	0.167	0.09
3b	0.271	0.750	0.178	0.346	1.62	0.225	0.09
3c	0.271	0.750	0.215	0.418	1.96	0.272	0.09
4a	0.308	0.853	0.085	0.150	0.63	0.081	0.10
4b	0.308	0.853	0.137	0.242	1.01	0.130	0.10
4c	0.308	0.853	0.182	0.322	1.34	0.173	0.10
4d	0.308	0.853	0.250	0.442	1.84	0.237	0.10
4e	0.308	0.853	0.296	0.523	2.18	0.281	0.10
5a	0.374	1.036	0.122	0.189	0.66	0.078	0.12
5b	0.374	1.036	0.205	0.318	1.11	0.131	0.12
5c	0.374	1.036	0.286	0.444	1.55	0.183	0.12
5d	0.374	1.036	0.385	0.597	2.08	0.247	0.12
5e	0.374	1.036	0.402	0.623	2.17	0.257	0.12
6a	0.481	1.332	0.186	0.252	0.70	0.079	0.15
6b	0.481	1.332	0.317	0.429	1.19	0.135	0.15
6c	0.481	1.332	0.438	0.593	1.64	0.187	0.15
(*)	0.481	1.332	0.530	0.718	1.99	0.226	0.15
7a	0.684	1.894	0.391	0.470	0.94	0.117	0.22
7b	0.684	1.894	0.572	0.688	1.37	0.171	0.22
(*)	0.631	1.745	0.683	0.838	1.64	0.204	0.22
8	0.917	2.536	0.631	0.724	1.09	0.166	0.29
(*)	0.917	2.536	0.806	0.925	1.40	0.212	0.29

Table 1: Parameters for the test cases used in this work, and thus also the experiments conducted by Kriebel (1992). The figure numbers correspond to the figures in this work. An asterisk denotes an experiment where wave breaking or vertical jetting was observed.

computed correct to second order by first solving the linear problem and then using this result as input to the second-order problem. The linear results are compared with the well known linear diffraction theory solution by MacCamy and Fuchs (1954), while the second-order results are compared with the semi-analytical solution and with experimental results – both by Kriebel (1992). All the test cases from Kriebel (1992) have been reproduced in the present work and good agreement is found between the results of the two numerical models for all cases considered here. (see Figures 3 to 8). In the figures the BEM results for the linear run-up are shown with dashed lines and the second-order run-up with solid lines. The analytical linear run-up (*i.e.* the MacCamy and Fuchs solution) is shown with crosses and the second-order semi-analytical solution with diamonds. Experimental results are shown with squares. Due to symmetry only the run-up around half the circumference of the cylinder is depicted.

The agreement between the two linear solutions is excellent for all cases considered. For the maximum run-up on the cylinder the difference between the results of the present linear time domain BEM and the ditto analytical solution is less than 0.5%.

The agreement between the BEM and the semi-analytical second-order run-up by Kriebel (1992) is also good. It can be seen for all cases that the second-order wave run-up is sig-

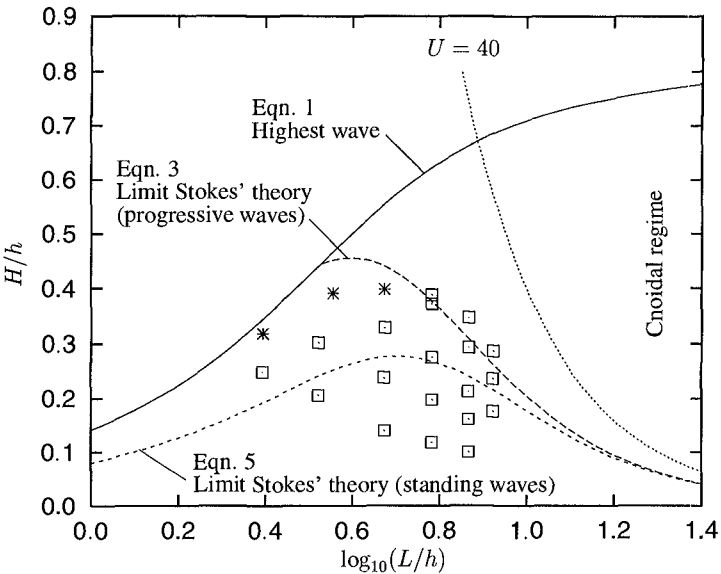


Figure 2: Scatter diagram of the experiments by Kriebel (1992) used in this work (\square) and experiments with observed wave breaking or vertical jetting ($*$). Also shown is the highest wave (Fenton, 1990) (—), the limit for Stokes' second-order progressive waves (---), the limit for Stokes' second-order standing waves (-·-·-), and the Ursell number $U=40$ (.....).

nificantly larger than the linear wave run-up. For assessment of wave overtopping or deck slamming on gravity-based bottom mounted structures this is of significant importance.

The experimental results by Kriebel (1992) show larger run-up both on the front and on the lee side of the cylinder than predicted by linear theory. Thus significant non-linear diffraction effects are represented in the experimental data. The second-order results compare reasonably well with the experiments in all but the most severe cases (see Figs. 4d-e, 5d-e and 7b). It should be noted that in all these latter cases the "no secondary crest condition" for second-order standing waves (5) has been violated.

A vertical cross-section of a wave envelope in the direction of the main wave propagation direction is shown in Figure 9 as an example of the good agreement between the 3D BEM and the semi-analytical second-order solution in the fluid domain away from the cylinder. The cross-section is taken along the x -axis, *i.e.* with $y = 0$ (see Fig. 1.) It is noted from the figure that the agreement is good even though a fairly small computational domain has been used for the time domain BEM.

6 CONCLUSIONS

A comparison has been made between the 3D second-order time domain Boundary Element Model by Büchmann *et al.* (1998) and the second-order semi-analytical frequency domain solution by Kriebel (1990) for calculation of run-up on a large vertical circular bottom mounted cylinder. Good agreement has been found between results from the two models.

Comparison between the second-order results and the experimental results by Kriebel (1992) show reasonably good agreement except in cases with strongly non-linear waves. By comparing with solutions of the linear wave diffraction problem, it is demonstrated that second-order effects are important for assessment of *e.g.* wave overtopping or deck slamming on gravity based bottom mounted structures.

7 ACKNOWLEDGEMENTS

This work was funded in part by the Danish National Research Foundation.

REFERENCES

- Büchmann, B., Skourup, J. and Cheung, K. F., (1998). Run-up on a structure due to second-order waves and a current in a numerical wave tank. To appear in *Applied Ocean Research*.
- Fenton, J. D., (1990). Nonlinear wave theories. *The Sea*, edited by B. Le Mehaute and D. M. Hanes, vol. 9, chap. 1, 5–25. John Wiley & Sons, New York.
- Kriebel, D. L., (1990). Nonlinear wave interaction with a vertical circular cylinder. Part I: Diffraction theory. *Ocean Engineering*, **17**(4), 345–377.
- Kriebel, D. L., (1992). Nonlinear wave interaction with a vertical circular cylinder. Part II: Wave run-up. *Ocean Engineering*, **19**(1), 75–99.

MacCamy, R. C. and Fuchs, R. A., (1954). Wave forces on piles: A diffraction theory. Tech. Memo. 69, U.S. Army Corps of Engineers, Beach Erosion Board, Washington D.C.

Skourup, J., (1996). Active absorption in a numerical wave tank. *Proceedings of the 6th International Offshore and Polar Engineering Conference*, vol. 3, 31–38, Los Angeles, USA.

Skourup, J. and Bingham, H. B., (1996). Active absorption of radiated waves in a 3D boundary element model. *Proceedings of the 11th International Workshop on Water Waves and Floating Bodies*, Hamburg, Germany.

Svendsen, I. A. and Jonsson, I. G., (1980). *Hydrodynamics of Coastal Regions*. Den Private Ingeniørfond, Technical University of Denmark, 2nd edn.

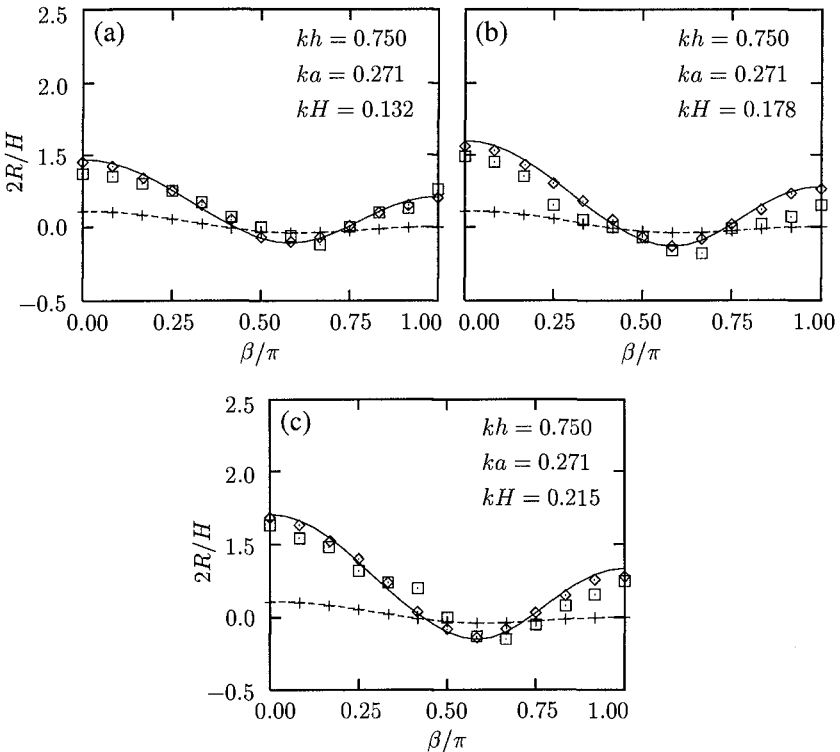


Figure 3: Run-up, R , as function of the angle, β , around a cylinder for $kh = 0.750$ and $ka = 0.271$. Numerical results to first order (---) and to second order (—). Analytical results by MacCamy and Fuchs (1954) (+). Semi-analytical results (\diamond) and experimental results (\square) by Kriebel (1992).

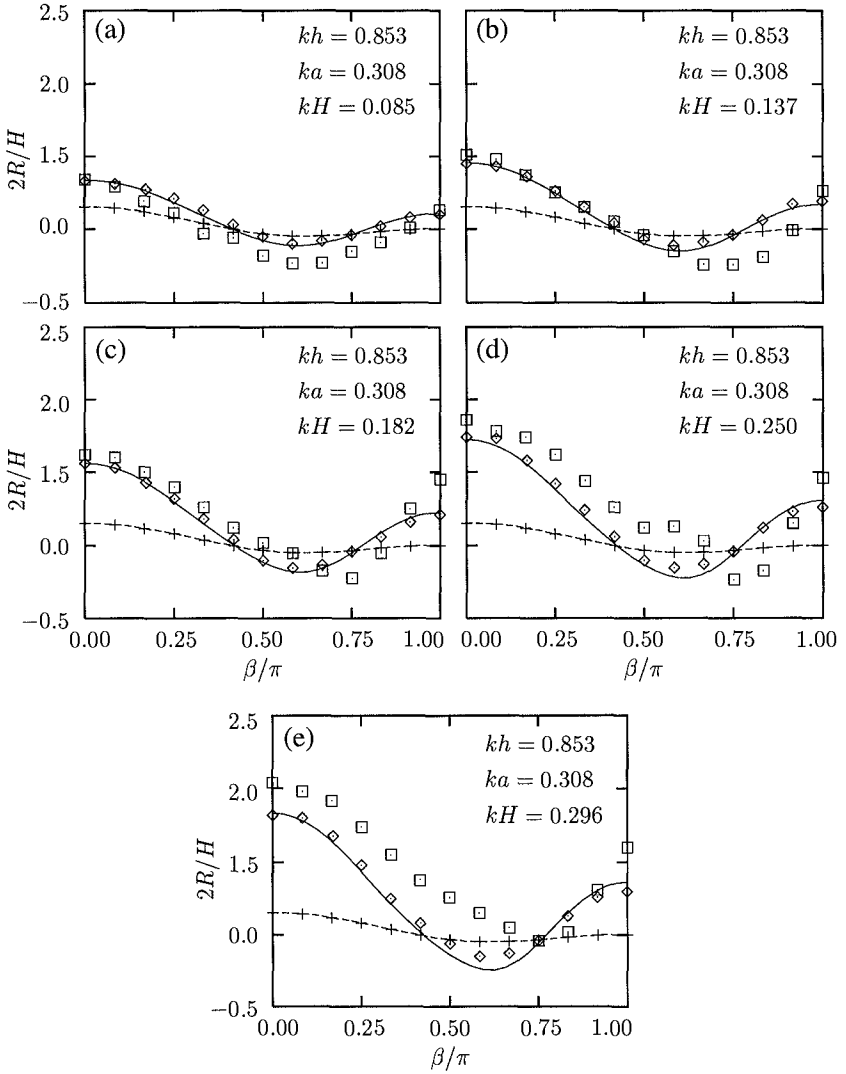


Figure 4: Run-up, R , as function of the angle, β , around a cylinder for $kh = 0.853$ and $ka = 0.308$. Numerical results to first order (---) and to second order (—). Analytical results by MacCamy and Fuchs (1954) (+). Semi-analytical results (\diamond) and experimental results (\square) by Kriebel (1992).

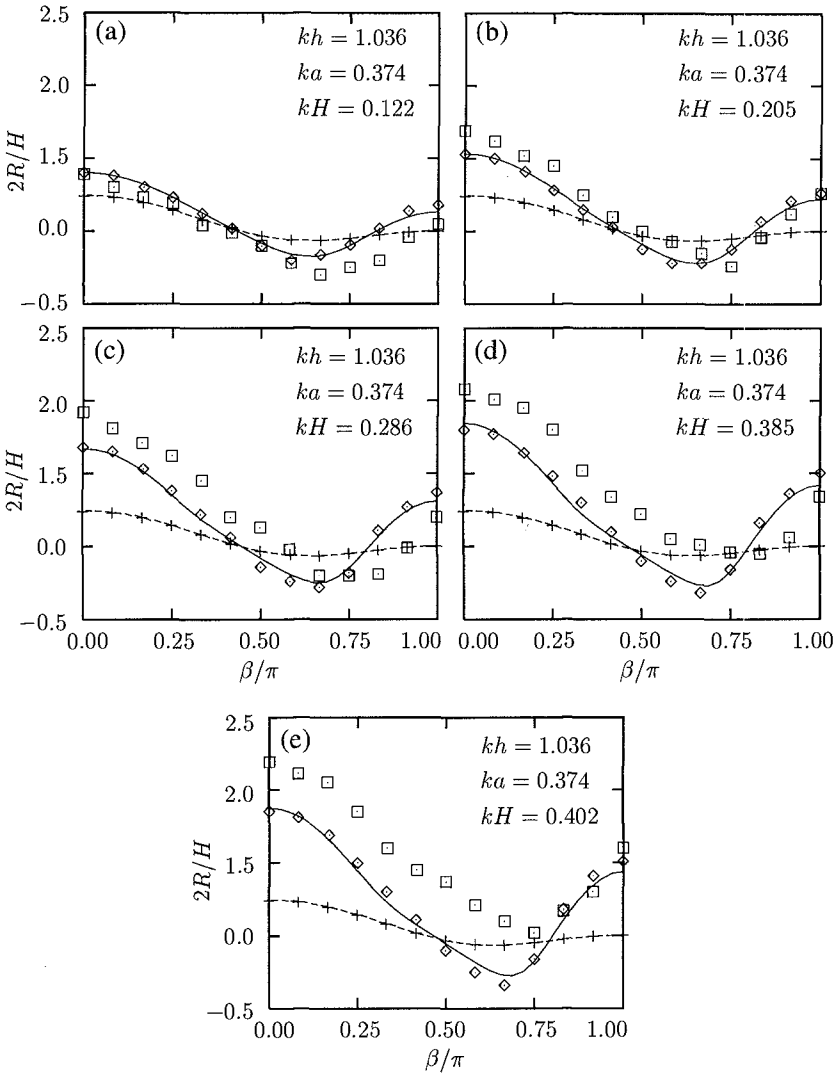


Figure 5: Run-up, R , as function of the angle, β , around a cylinder for $kh = 1.036$ and $ka = 0.374$. Numerical results to first order (---) and to second order (—). Analytical results by MacCamy and Fuchs (1954) (+). Semi-analytical results (o) and experimental results (□) by Kriebel (1992).

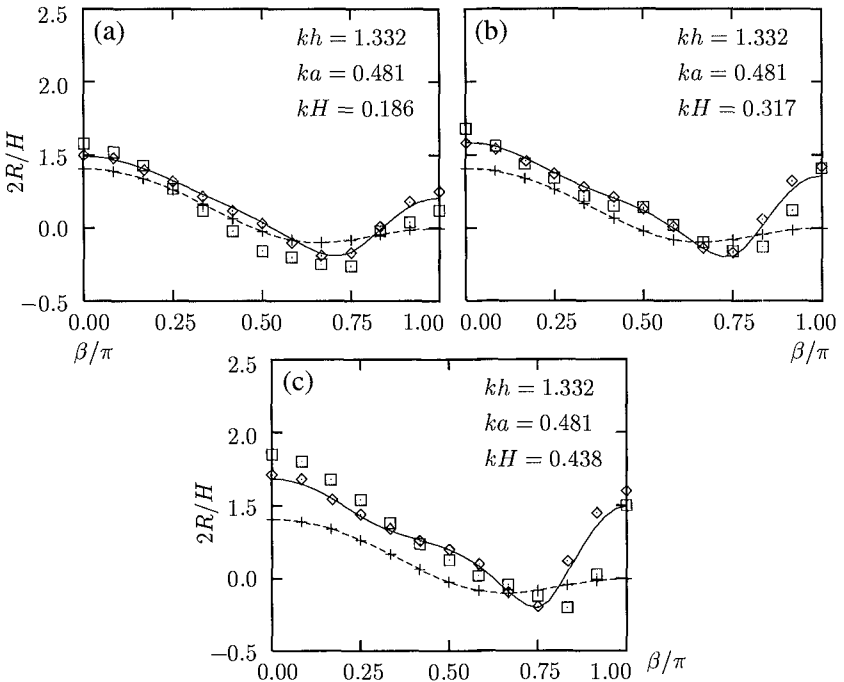


Figure 6: Run-up, R , as function of the angle, β , around a cylinder for $kh = 1.332$ and $ka = 0.481$. Numerical results to first order (---) and to second order (—). Analytical results by MacCamy and Fuchs (1954) (+). Semi-analytical results (\diamond) and experimental results (\square) by Kriebel (1992).

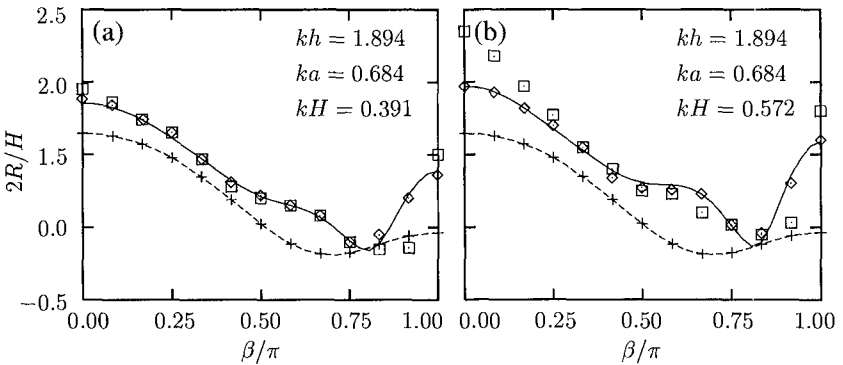


Figure 7: Run-up, R , as function of the angle, β , around a cylinder for $kh = 1.894$ and $ka = 0.684$. Legend: see Fig. 6 above.

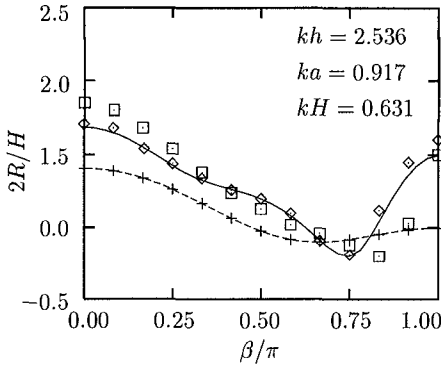


Figure 8: Run-up, R , as function of the angle, β , around a cylinder for $kh = 2.536$ and $ka = 0.917$. Numerical results to first order (---) and to second order (—). Analytical results by MacCamy and Fuchs (1954) (+). Semi-analytical results (\diamond) and experimental results (\square) by Kriebel (1992).

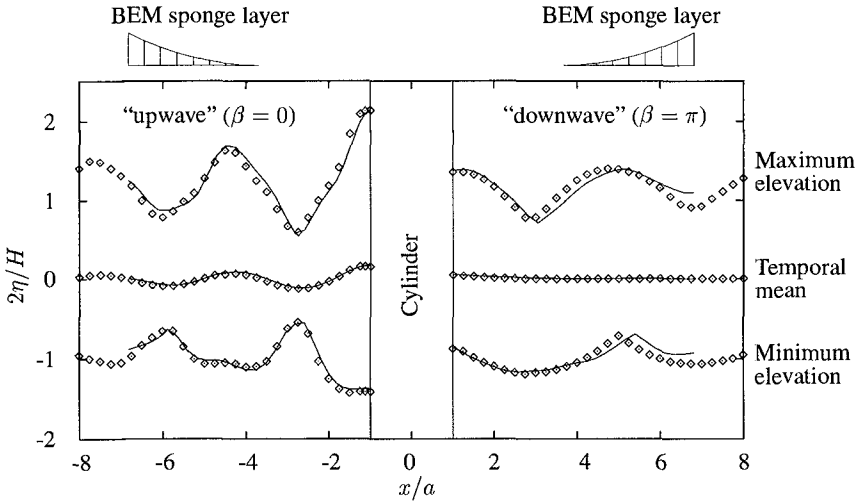


Figure 9: Vertical cross-section of wave envelope in the direction of wave propagation consistent to second order with $ka = 1.00$, $kh = 1.57$ and $kH = 0.50$. Numerical results using the BEM (—) and semi-analytical results by Kriebel (1990) (\diamond). The spatial extent of the BEM is indicated by the sponge layers.